Accepted Manuscript

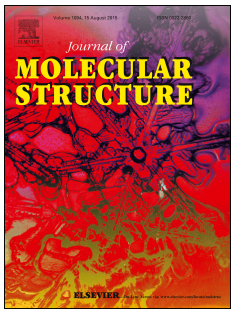

Experimental and theoretical investigation on conformational and spectroscopic properties of dimethyl dithiodiglycolate, $[CH_3OC(O)CH_2S]_2$

Luciana C. Juncal, Yanina B. Bava, Luciana M. Tamone, Samantha Seng, Yeny A. Tobón, Sophie Sobanska, A. Lorena Picone, Rosana M. Romano

PII: S0022-2860(17)30204-1

DOI: 10.1016/j.molstruc.2017.02.058

Reference: MOLSTR 23452

To appear in: *Journal of Molecular Structure*

Received Date: 18 January 2017

Revised Date: 11 February 2017

Accepted Date: 13 February 2017

Please cite this article as: L.C. Juncal, Y.B. Bava, L.M. Tamone, S. Seng, Y.A. Tobón, S. Sobanska, A.L. Picone, R.M. Romano, Experimental and theoretical investigation on conformational and spectroscopic properties of dimethyl dithiodiglycolate, $[CH_3OC(O)CH_2S]_2$, *Journal of Molecular Structure* (2017), doi: 10.1016/j.molstruc.2017.02.058.

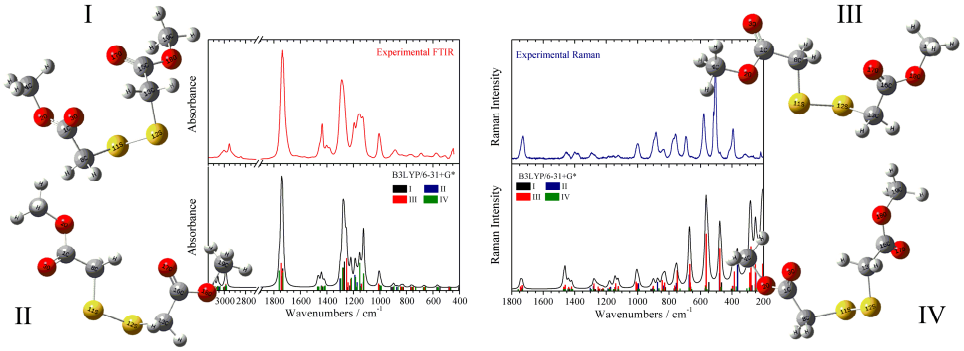

Experimental and theoretical investigation on conformational and spectroscopic properties of dimethyl dithiodiglycolate, $[CH_3OC(O)CH_2S]_2$

Luciana C. Juncal,[†] Yanina B. Bava,[†] Luciana M. Tamone,[†] Samantha Seng,[‡] Yeny A. Tobón,[‡] Sophie Sobanska,[‡,§] A. Lorena Picone,[†] Rosana M. Romano[,†]*

[†] CEQUINOR (UNLP, CCT-CONICET La Plata). Departamento de Química, Facultad de Ciencias Exactas, Universidad Nacional de La Plata. Blvd. 120 N° 1465, La Plata (CP 1900), Argentina.

[‡] Laboratoire de Spectrochimie Infrarouge et Raman, UMR CNRS 8516, Université de Lille 1 Sciences et Technologies, Bât. C5, 59655 Villeneuve d'Ascq Cedex, France.

[§] Present address: Institut des Sciences Moléculaires, Université de Bordeaux, CNRS UMR 5255, Bâtiment A12, 351 cours de la libération, 33405 Talence cedex, France

AUTHOR EMAIL ADDRESS: romano@quimica.unlp.edu.ar

Abstract

Dimethyl dithiodiglycolate (DTG), $[CH_3OC(O)CH_2S]_2$, was synthetized by complete oxidation of methyl thioglycolate (MTG) with I_2, and characterized by gas chromatography coupled with electron-impact mass spectrometry. Fifteen stable conformers were found with the B3LYP/6-31+G* approximation, with calculated populations at ambient temperature higher than 1 %. The IR and Raman spectra of liquid DTG were interpreted for the first time, in terms of equilibrium between four conformers. The UV-visible spectra of DTG in solutions of ethanol, isopropanol and acetonitrile present a low-intensity band around 230 nm, interpreted mainly as arising from $n \rightarrow \pi^*$ transitions localized at the C=O groups, according to the prediction of TD-DFT calculations.

Introduction

Recently, dimethyl dithiodiglycolate (DTG), $[CH_3OC(O)CH_2S]_2$, was proposed to be formed from methyl thioglycolate (MTG), $CH_3OC(O)CH_2SH$, in levitated microdroplets exposed to ambient air [1]. The transformation was followed by microRaman spectroscopy, clearly evidenced by the development of a new Raman band assigned to the disulfide stretching vibrational mode, together with the intensity decrease of the Raman band associated with the S–H vibrational mode. Subsequent irradiation with monochromatic light of 325 nm in ambient air conducts to formation of sulfate (SO_4^{2-}) and elemental sulfur (α-S_8), undoubtedly recognized by their Raman characteristic bands. To the best of our knowledge, the spectroscopic characterization of DTG was not performed so far.

DTG was first reported in Ref. [2], in which the oxidation mechanisms of different thiols by iodine were studied. A few years later, its desulfurization mechanism on treatment with aminophosphines was studied, but no characterization of this compound was reported [3]. DTG was also identified as a by-product of the telomerization of acrylic acid with thioglycolic acid in aqueous medium, with different initiators like H_2O_2 and $S_2O_8^{2-}$ [4]. Recently, DTG was found as a product of the reaction of methylthioglycolate (MTG) and iodine during the preparation of an iodine-molecule-coordinated octanuclear palladium thiolate complex, $[Pd(\mu\text{-}SCH_2CO_2CH_3)_2]_8$, but no complete characterization of this disulfide was achieved [5].

In this paper we present a structural and conformational study of DTG, $[CH_3OC(O)CH_2S]_2$, based on vibrational spectroscopies (IR and Raman) and DFT methods. The UV-visible spectra were measured in solutions of different solvents, and interpreted on the basis of TD-DFT calculations. The molecule was synthetized by complete oxidation of MTG with iodine in alkaline media, and characterized by gas chromatography coupled with mass spectrometry.

Experimental section

Synthesis. Reagents (MTG, iodine and KOH) and solvents ($CH_3CH_2OCH_2CH_3$, CH_3CH_2OH, $(CH_3)_2CHOH$, $CHCl_3$ and CH_3CN) were purchased reagent grade. Solvents were dried with molecular sieves before used. Dimethyl dithiodiglycolate, $[CH_3OC(O)CH_2S]_2$, was synthesized by the oxidation of MTG according to the literature procedure, described by eq. 1 [5-7]. Iodine was added to an alkaline solution of MTG in acetonitrile. The reactants were mixed at room temperature, and the reaction mixtures were stirred during 1 h. DTG was obtained as pale yellow oil and purified by successive extractions using diethyl ether. The final purity of the compound was checked by GC-MS and FTIR.

$$2\ CH_3OC(O)CH_2SH + I_2 + 2\ KOH \longrightarrow CH_3OC(O)CH_2SSCH_2C(O)OCH_3 + 2\ KI + 2\ H_2O \qquad (1)$$

Gas chromatography - mass spectrometry. The GC-MS analysis was carried out on a Shimadzu QP-2010. Details are given in Table S1 of the Supplementary Material.

FTIR spectroscopy. The FTIR spectra were recorded at room temperature on an Equinox 55 Bruker instrument equipped with an MCTB detector, with a resolution of 4 cm^{-1}. The IR spectra of the neat liquid were measured between KBr windows, to cover the range between 4000 and 400 cm^{-1}.

Raman spectroscopy. The Raman spectra were measured in a dispersive Horiba-Jobin-Yvon T64000 Raman spectrometer, with a confocal microscope and CCD detection. The wavenumbers were calibrated with the 459 cm^{-1} band of CCl_4. The sample, placed in a sealed 2 mm glass capillary, was excited with a 514.5 nm light from an Ar multiline laser.

UV-visible spectroscopy. UV-visible spectra in the 200-800 nm range of solutions of the sample in solvents of different polarity, ethanol, isopropanol and acetonitrile, and at different concentrations were recorded at room temperature on a Shimadzu UV-2600 spectrometer using a 1 cm-quartz cell. The absorption coefficient (ε) was calculated by a linear regression of the plot of the UV-visible absorbance against the molar concentration.

Theoretical calculations. All quantum chemical calculations were performed with the Gaussian 03 program system [8], using the B3LYP method in combination with a 6-31+G* basis set. Potential energy curves for the internal rotation of selected dihedral angles were calculated to evaluate the conformational equilibrium using the B3LYP/6-31+G* approximation. Geometry optimizations of all possible conformers were sought using standard gradient techniques by simultaneous relaxation of all the geometrical parameters. The calculated vibrational properties correspond in all cases to potential energy minima for which no imaginary vibrational frequency was

found. Relative Raman Intensities were obtained from the Raman activities given by the Gaussian calculation as reported before by Krishnakumar et al., with the help of GaussSum 3.0 program [9,10]. The electronic spectrum was simulated using the TD-DFT formalisms over the previously optimized structures, with a maximum of 100 states and S = 1 [11,12].

Results and discussion

Gas chromatography and Mass spectrometry. Figure 1 shows the mass spectrum of DTG obtained from CCl_4 solutions of approximately 200 ppm. In the conditions specified in Table S1, the elution time was 8.8 minutes for $[CH_3OC(O)CH_2S]_2$. The most intense peaks observed in the 70 eV electron-impact mass spectrum correspond to m/z = 45 (CSH^+ or $COOH^+$, 100%), m/z = 15 (CH_3^+, ~45%), m/z = 59 ($C(O)OCH_3^+$, ~36%) and m/z = 46 (CH_2S^+, ~32%). The peak at m/z = 106 corresponds to $CH_3OC(O)CH_2SH^{+\bullet}$ (~12%); this odd-electron ion appears due to an hydrogen rearrangement followed by the loss of the $CH_3OC(O)CHS$ neutral fragment, as shown in Scheme I. This mechanism is also able to explain the m/z = 46 peak assigned to CH_2S^+, previously reported for MTG fragmentation upon electron impact ionization [13]. The parent ion M^+ (m/z = 210) was also detected with an abundance around 15 %, with its characteristic isotopic pattern. A complete list of the peaks observed in the mass spectrum of $[CH_3OC(O)CH_2S]_2$, together with their relative abundances and assignments is presented as supplementary material (Table S2). Figure S1 depicts selected fragmentation mechanisms of DTG after electron-impact ionization.

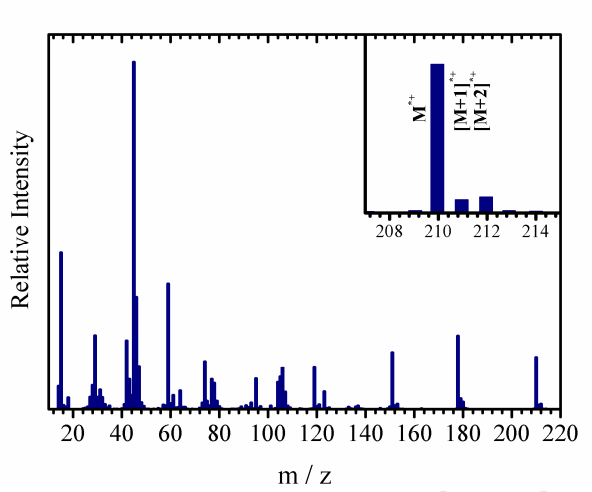

Figure 1. Mass spectrum of $[CH_3OC(O)CH_2S]_2$ obtained from a CCl_4 solution at 70 eV electron-impact ionization.

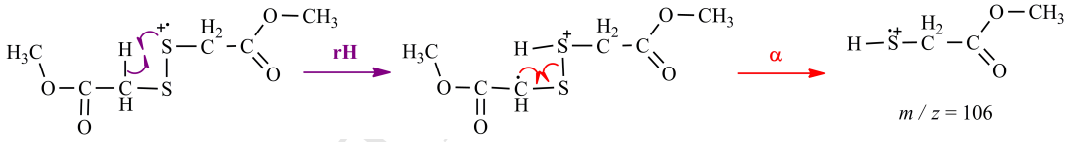

Scheme I. Proposed atomic rearrangement mechanism to explain the formation of the m/z = 106 fragment.

Theoretical calculations. The structures and conformations of the DTG molecule were theoretically investigated using a DFT (B3LYP) method, mainly to help in the interpretation of the vibrational spectra in terms of different possible conformers in equilibrium.

A large number of conformations can be considered for DTG, accessible through internal rotation around the C–O (τ_1, τ_5), C–C (τ_2, τ_4) or S–S (τ_3) single bonds (see Scheme II). To start the conformational analysis, five relaxed potential energy scans, one for each of the considered dihedral angles, were performed. The potential energy curves calculated for τ_1 and τ_5 (C–O–C=O), depicted in Figure S2 of the supplementary material, present two minima, at 0 and 180 º, respectively. A preferred planar conformation of the $CH_3OC(O)$– group is in agreement with results obtained for related molecules [14-16].

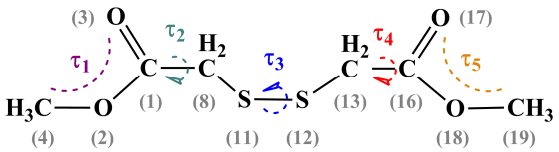

Scheme II. Schematic representation of the dihedral angles (τ_1-τ_5) taken into account for the conformational study of $[CH_3OC(O)CH_2S]_2$.

Two minima were also found in the potential energy curves obtained when τ_2 and τ_4 (O=C–C–S) were varied, occurring at 110 and 270 º (see Figure S2). The last scan was performed for τ_3 (C–S–S–C), in which the typical conformations of a disulfide molecule, i.e. *gauche* and *–gauche* forms [17,18], were found as minima (see Figure S2). Considering these results, a total of 2^5 = 32 possible conformations are feasible. All these possible structures were explored by using the B3LYP/6-31+G* approximation. Taking into account for the discussion only those conformers laying 3 Kcal/mol or less above the most stable structure, fifteen conformers were found as minima of the potential energy surface, for which no imaginary frequencies occur. The molecular models of these DTG rotamers are shown in Figure S3, while the relevant dihedral angles and predicted energy differences (corrected by zero-point

energy) together with the percentage of each form calculated at ambient temperature are presented in Table S3. The molecular models of the four most stable conformers (I-IV) are depicted in Figure 2.

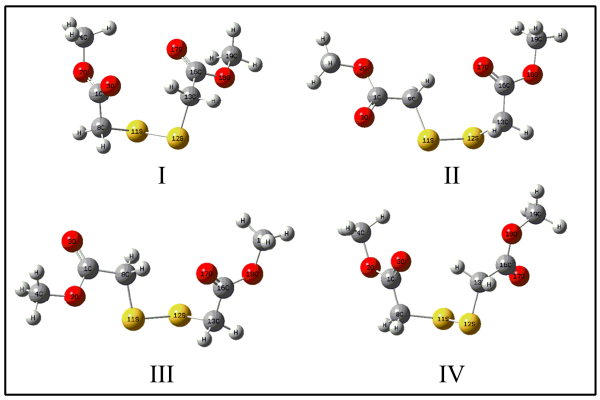

Figure 2. Molecular models of the four most stable conformers of $[CH_3OC(O)CH_2S]_2$ calculated with the B3LYP/6-31+G* approximation.

The different conformers can be classified into three groups, according to their energy differences. The first group, composed of conformers (I-V) with potential energy differences below 1 Kcal/mol, corresponds to a population around 66 % at ambient temperature. The second group, formed by structures VI–X with energy differences between 1.3–1.9 Kcal/mol with respect to the most stable form (structure I), represents almost 17 % of the total population. The last five structures (XI–XV), with computed energy differences between 2.1 and 2.7 Kcal/mol with respect to form I, corresponds to 16 % of the population.

Vibrational analysis. Figure 3 shows the FTIR and Raman spectra of a liquid sample of DTG and Table 1 lists selected wavenumbers observed in these spectra. The assignment of the bands has been performed with the aid of the predictions of

theoretical calculations and also by the comparison with related molecules, mainly MTG.[Error! Bookmark not defined.] The vibrational spectra (IR and Raman) were simulated for each of the conformers to help in the interpretation of the experimental spectra. From the comparative analysis of the theoretical wavenumbers and relative IR and Raman intensities of the conformers we can conclude that some of the vibrational modes are sensitive to the conformation adopted by the molecules. Although the calculations were performed for the isolated molecule, and therefore ignoring the intermolecular interactions present in the liquid phase, the agreement between the experimental and theoretical spectra is very good. Figures S4 and S5 present the comparison between the experimental IR and Raman spectra with the theoretical spectra of a weighted mixture of the different conformers. The calculated IR and Raman spectra were reproduced using Gaussian line shapes and a full width at half maximum (FWHM) of 15 cm^{-1} in order to obtain a better correlation with the experimental results.

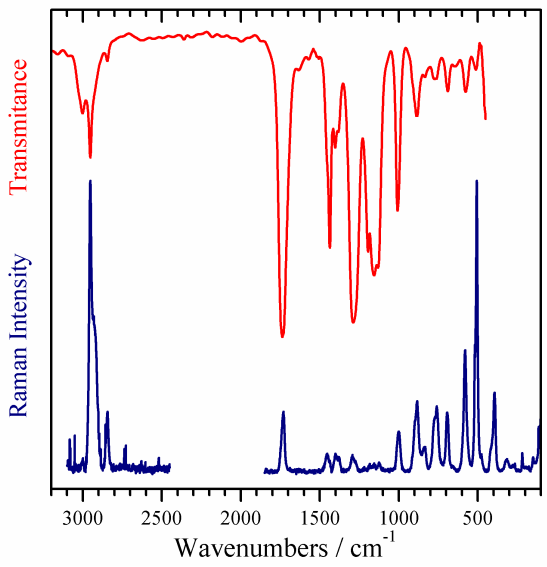

Figure 3. FTIR (upper red trace, between 3200 and 400 cm^{-1}) and Raman (lower blue trace, between 3200 and 100 cm^{-1}) spectra of liquid $[CH_3OC(O)CH_2S]_2$.

Table 1. Experimental wavenumbers (cm^{-1}) of selected FTIR and Raman bands of $[CH_3OC(O)CH_2S]_2$, calculated normal modes for the most stable conformers (relative populations are given in parentheses), and tentative assignment

Experimental		B3LYP/6-31+G*[a]				Tentative Assignment
FTIR	Raman	I (17.0%)	II (10.2%)	III (19.2%)	IV (16.1 %)	
					1759	ν (C=O) [IV]
			1742	1745		ν (C=O) [II, III]
1730	1730	1734		1735		ν (C=O) [I, III]
		1732	1732		1732	ν (C=O) [I, II, IV]
1294	1290		1302		1295	ν_{as} C–C–O [II, IV]
1279			1281		1281	ν_{as} C–C–O [II, IV]
1273	1275	1277		1278		ν_{as} C–C–O [I, III]
		1268				ν_{as} C–C–O [I]
1009	1001	1009		1010		ν O–CH_3 [I, III]
997		1003	1001	1003	1001	ν O–CH_3 [I-IV]
					894	δ_{oop} C=O [IV]
885	883		874		865	ν_s C–C–O [II, IV]
	839			844		ν_s C–C–O [III]
			835		837	ν_s C–C–O [II, IV]
835		825		828		ν_s C–C–O [I, III]
		824				ν_s C–C–O [I]
780		768		764		δ_{oop} C=O [I, III]
	776	761	759			δ_{oop} C=O [I, II]
760			755		755	δ_{oop} C=O; ν C–S [II, IV]
	758			749		ν C–S [III]
	693	671			673	δ CCO [I, IV]
689		663	667	665		δ OCO [I, II, III]

Experimental		B3LYP/6-31+G*[a]				Tentative Assignment
FTIR	Raman	I (17.0%)	II (10.2%)	III (19.2%)	IV (16.1 %)	
579	580	565	565	565	567	ν C–S [IV] ν C–S ; δ CCO [I, II, III]
511	519		480	478		ν S–S [II, III]
	506	467			469	ν S–S [I, IV]
	476	404 406				δ CCO [I]
	418		395	397	396	δ CCO [II, III, IV]
	393		365	386	374	δ COC [II, III, IV]
	317		288	287	306	
	274	281	249	251	246	δ CCS [I-IV]

[a] scaled by the 0.97 factor [19].

As can be observed in Table 1, some of the vibrational modes are sensitive to the conformation adopted by the molecule, and the experimental IR and Raman spectra can only be fully interpreted taken into account the contribution of the different rotamers. The most intense absorption in the IR spectrum of DTG occurs at 1730 cm^{-1} as a wide band, and is assigned to the ν C=O vibrational modes of the different conformers. According to the prediction of the performed calculations for the wavenumber differences and relative intensities of these vibrational modes for the four most stable conformers (two for each conformer, i.e. eight modes in total), a wide an unresolved band is expected. Figure S6 of the supplementary material compares the IR and Raman spectra in the ν C=O region, with the weighted sum of the theoretical spectra of each form.

The second most intense feature in the IR spectrum appears at 1279 cm^{-1}, and can be assigned, together with the unresolved shoulder at lower wavenumbers, to the C–C–O antisymmetric stretching mode. The symmetric ν C–C–O mode is sensitive to the conformation adopted by the molecule; two different bands, at 885 (conformers II and IV) and 835 cm^{-1} (conformers I and III), could be assigned to this vibrational mode, in accordance with theoretical predictions (see Table 1).

The most intense bands of the Raman spectrum of $[CH_3OC(O)CH_2S]_2$ correspond to the C–H stretching modes of the methyl and methylene groups of the molecule, followed by the S–S stretching normal mode, occurring at 506 cm^{-1} with a well-defined shoulder at 519 cm^{-1}. The former band is assigned to conformers I and IV, while the shoulder corresponds to conformers II and III.

Figure 4 compares selected regions of the experimental IR and Raman spectra with the simulated ones using the B3LYP/6-31+G* approximation, composed by a weighted sum of the spectra of each conformer. As can be observed in this figure, the complicated pattern of the infrared and Raman spectra can only be completely explained by the presence of the four considered conformers. A complete list of the IR and Raman experimental bands together with the predicted ones at B3LYP/6-31+G* level of theory for each of the lower energy conformers and the proposed assignment is presented in Table S4.

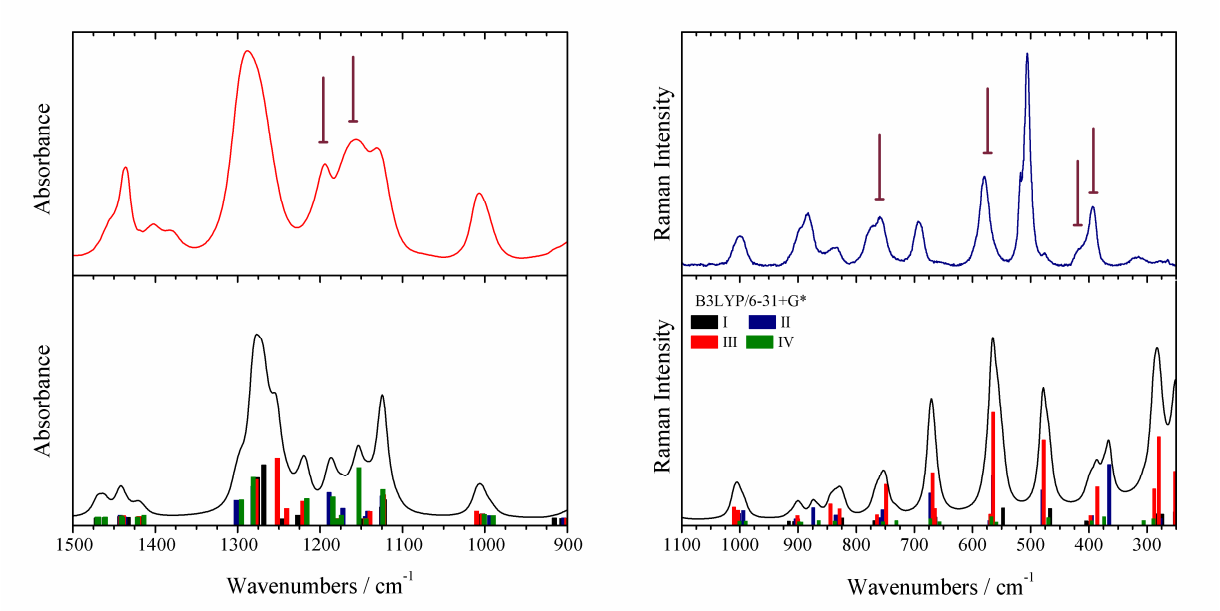

Figure 4. Experimental FTIR (upper red trace) and Raman spectra (upper blue trace) of liquid $[CH_3OC(O)CH_2S]_2$ and weighted sum of the computed spectra for the four most stable forms of DTG calculated with the B3LYP/6-31+G* approximation (lower black trace). The absorbance or Raman intensity of the normal modes for the four most stables conformers are shown in bars.

Electronic absorption spectroscopy. The UV-visible spectra of DTG in solutions of different solvents (ethanol, isopropanol and acetonitrile) were measured at various concentrations. To help in the interpretation and assignment of the UV-visible spectra, TD-DFT calculations were performed using the B3LYP/6-31+G* approximation. The calculated spectrum is characterized by three bands, as can be observed in Figure 5. The experimental UV-visible spectra of DTG in ethanol and isopropanol solutions are also shown in the figure. The low intensity absorption, close to 230 nm (ε ~1210 $L.mol^{-1}.cm^{-1}$) for the spectrum taken in ethanol solution, near 236 nm (ε ~860 $L.mol^{-1}.cm^{-1}$) in the isopropanol solution, and around 230 nm for the acetonitrile solution, is assigned to $n \rightarrow \pi^*$ transitions localized at the C=O

groups. Two intense absorptions are found around 165 and 145 nm and assigned to *n* → π* and *π* → π* transitions localized at the –OC(O)– groups, according to the TD-DFT calculations.

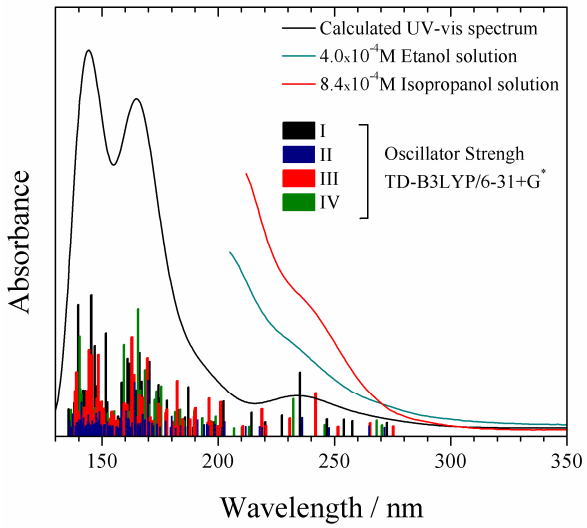

Figure 5. Experimental absorption spectra of DTG (in CH_3CH_2OH, light blue trace, and $(CH_3)_3CHOH$, red trace), theoretical UV-visible spectrum (black trace) and oscillator strength of the electronic transitions calculated for the four most stable conformers of $[CH_3OC(O)CH_2S]_2$ with the TD-B3LYP/6-31+G* approximation (bars).

Conclusions

The conformational analysis of dimethyl dithiodiglycolate (DTG), $[CH_3OC(O)CH_2S]_2$, was performed using theoretical methods and spectroscopic techniques. The preferred *gauche* (~ ±90°) conformation around the S–S single bond

and *syn* (~ 0°) for both CH_3–O–C=O dihedral angles were predicted by B3LYP/6-31+G* calculations. On the other hand, different values for both O=C–CH_2–S dihedral angles are feasible, giving a total of fifteen conformations with predicted populations higher than 1 % at ambient temperature. Although the calculations were performed for the free molecule, the experimental IR and Raman spectra of liquid DTG can only be fully interpreted by the presence of the four most stable conformers. The UV-visible spectra present a low-intensity band around 230 nm, that was interpreted by the aid of TD-DFT calculations as arising mainly from $n \rightarrow \pi^*$ transitions localized at the C=O groups. These transitions may be the responsible for the rich photochemistry of DTG as observed in levitation conditions [1].

Acknowledgement

The authors thank the Consejo Nacional de Investigaciones Científicas y Técnicas (CONICET) (PIP-0352), the Agencia Nacional Científica y Tecnológica (PICT11-0647 and PICT14-3266), the Facultad de Ciencias Exactas, Universidad Nacional de La Plata (UNLP-11/X684) and the international cooperation program ECOS-MinCyT (A13E05) for financial support.

REFERENCES

[1] Y.A. Tobón, S. Seng, A.L. Picone, Y.B. Bava, L.C. Juncal, M. Moreau, R.M. Romano, J. Barbillat, S. Sobanska, Photochemistry of single particles using

acoustic levitation coupled with Raman microspectrometry, submitted to J. Raman Spectrosc.

[2] J.P. Danehy, M.Y. Oester, Oxidation of organic divalent sulfur by iodine. I. Alternative pathways for thiols as determined by structure, J. Org. Chem. 32 (1967) 1491–1495. doi:10.1021/jo01280a041.

[3] D.N. Harpp, J.G. Gleason, Organic sulfur chemistry. X. Selective desulfurization of disulfides. Scope and mechanism, J. Am. Chem. Soc. 93 (1971) 2437–2445. doi:10.1021/ja00739a014.

[4] B. Boutevin, G. Rigal, M. El Asri, T. Lakhlifi, Tklomkrisation en milieu aqueux, Macromol. Chem. Phys. 196 (1995) 2303–2319. doi:10.1002/macp.1995.021960718.

[5] Y. Yamashina, Y. Kataoka, Y. Ura, Inclusion of an iodine molecule in a tiara-like octanuclear palladium thiolate complex, Eur. J. Inorg. Chem. 2014 (2014) 4073–4078. doi:10.1002/ejic.201402616.

[6] B. Zeynizadeh, Oxidative coupling of thiols to disulfides with iodine in wet acetonitrile, J. Chem. Res. 2002 (2002) 564–566. doi:10.3184/030823402103170781.

[7] B. Mandal, B. Basu, Recent advances in S–S bond formation, RSC Adv. 4 (2014) 13854. doi:10.1039/c3ra45997g.

[8] M.J. Frisch, G.W. Trucks, H.B. Schlegel, G.E. Scuseria, M.A. Robb, J.R. Cheeseman, J.A. Montgomery, Jr., T. Vreven, K.N. Kudin, J.C. Burant, J.M. Millam, S.S. Iyengar, J. Tomasi, V. Barone, B. Mennucci, M. Cossi, G. Scalmani, N. Rega, G.A. Petersson, H. Nakatsuji, M. Hada, M. Ehara, K.

Toyota, R. Fukuda, J. Hasegawa, M. Ishida, T. Nakajima, Y. Honda, O. Kitao, H. Nakai, M. Klene, X. Li, J.E. Knox, H.P. Hratchian, J.B. Cross, C. Adamo, J. Jaramillo, R. Gomperts, R.E. Stratmann, O. Yazyev, A.J. Austin, R. Cammi, C. Pomelli, J.W. Ochterski, P.Y. Ayala, K. Morokuma, G.A. Voth, P. Salvador, J.J. Dannenberg, V.G. Zakrzewski, S. Dapprich, A.D. Daniels, M.C. Strain, O. Farkas, D.K. Malick, A.D. Rabuck, K. Raghavachari, J.B. Foresman, J.V. Ortiz, Q. Cui, A.G. Baboul, S. Clifford, J. Cioslowski, B.B. Stefanov, G. Liu, A. Liashenko, P. Piskorz, I. Komaromi, R.L. Martin, D.J. Fox, T. Keith, M.A. Al-Laham, C.Y. Peng, A. Nanayakkara, M. Challacombe, P.M.W. Gill, B. Johnson, W. Chen, M.W. Wong, C. Gonzalez, J.A. Pople, Gaussian 03, Revision B.01, Gaussian, Inc., Pittsburgh PA, 2003.

[9] V. Krishnakumar, G. Keresztury, T. Sundius, R. Ramasamy, Simulation of IR and Raman spectra based on scaled DFT force fields: a case study of 2-(methylthio)benzonitrile, with emphasis on band assignment, J. Mol. Struct. 702 (2004) 9–21. doi:10.1016/j.molstruc.2004.06.004.

[10] N.M. O'boyle, A.L. Tenderholt, K.M. Langner, cclib: A library for package-independent computational chemistry algorithms, J. Comput. Chem. 29 (2008) 839–845. doi:10.1002/jcc.20823.

[11] R. Bauernschmitt, R. Ahlrichs, Treatment of electronic excitations within the adiabatic approximation of time dependent density functional theory., Chem. Phys. Lett. 256 (1996) 454–464. doi:10.1016/0009-2614(96)00440-X.

[12] R.E. Stratmann, G.E. Scuseria, M.J. Frisch, An efficient implementation of time-dependent density-functional theory for the calculation of excitation

energies of large molecules, J. Chem. Phys. 109 (1998) 8218–8224. doi:10.1063/1.477483.

[13] O. Sekiguchi, S. Tajima, Fragmentation of organosulfur compounds upon electron impact. Part III. Metastable decomposition of the molecular ions of methyl thioglycolate and ethyl thioglycolate, J. Am. Soc. Mass Spectrom. 8 (1997) 801–808. doi:10.1016/S1044-0305(97)00079-2.

[14] Y.B. Bava, L.M. Tamone, L.C. Juncal, S. Seng, Y.A. Tobón Correa, A.L. Picone, R.M. Romano, Experimental and theoretical IR study of methyl thioglycolate, $CH_3OC(O)CH_2SH$, in different phases: evidence of a dimer formation, submitted to J. Mol. Struct.

[15] L.C. Juncal, M.V Cozzarín, R.M. Romano, Conformational and spectroscopic study of xanthogen ethyl formates, $ROC(S)SC(O)OCH_2CH_3$. Isolation of $CH_3CH_2OC(O)SH$, Spectrochim. Acta Part A Mol. Biomol. Spectrosc. 139 (2015) 346–355. doi:10.1016/j.saa.2014.12.086.

[16] Y.A. Tobón, H.E. Di Loreto, C.O. Della Védova, R.M. Romano, Matrix isolation study of ethyl chloroformate, $ClC(O)OCH_2CH_3$, J. Mol. Struct. 881 (2008) 139–145. doi:10.1016/j.molstruc.2007.09.007.

[17] L.C. Juncal, Y.A. Tobón, O.E. Piro, C.O. Della Védova, R.M. Romano, Structural, spectroscopic and theoretical studies on dixanthogens: $(ROC(S)S)_2$, with R = n-propyl and isopropyl, New J. Chem. 38 (2014) 3708. doi:10.1039/C4NJ00708E.

[18] A. Hermann, S.E. Ulic, C.O. Della Védova, H.-G. Mack, H. Oberhammer, Vibrational spectra and structures of halogencarbonyl alkyldisulfanes

XC(O)SSR with X=F, Cl and R=CF_3, CH_3, J. Fluor. Chem. 112 (2001) 297–305. doi:10.1016/S0022-1139(01)00515-2.

[19] A.P. Scott, L. Radom, Harmonic Vibrational Frequencies: An evaluation of Hartree−Fock, Møller−Plesset, quadratic configuration interaction, density functional theory, and semiempirical scale factors, J. Phys. Chem. 100 (1996) 16502–16513. doi: 10.1021/jp960976r.

Highlights

- Synthesis, isolation and characterization of DTG were achieved
- Vibrational spectra of DTG were interpreted by the presence of four conformers
- Fragmentation mechanisms of DTG after electron-impact ionization were proposed